Defining Amino Acid Residues Involved in DNA−Protein Interactions and Revelation of 3′-Exonuclease Activity in Endonuclease V†

Hong Feng, Liang Dong, Athena M. Klutz, Nima Aghaebrahim, and Weiguo Cao*

Department of Genetics, Biochemistry and Life Science Studies, South Carolina Experiment Station, Clemson University, Room 219, Biosystems Research Complex, 51 New Cherry Street, Clemson, South Carolina 29634

Received May 5, 2005; Revised Manuscript Received June 15, 2005

ABSTRACT: Endonuclease V is an enzyme that initiates a conserved DNA repair pathway by making an endonucleolytic incision at the 3′ side one nucleotide from a deaminated base lesion. Site-directed mutagenesis analysis was conducted at seven conserved motifs of the thermostable *Thermotoga maritima* endonuclease V to probe for residues that affect DNA−protein interactions. Y80, G83, and L85 in motif III, H116 and G121 in motif IV, A138 in motif V, and S182 in motif VI affect binding of both the double-stranded inosine-containing DNA substrate and the nicked double-stranded inosine-containing DNA product, resulting in multiple enzymatic turnovers. The substantially reduced DNA cleavage activity observed in G113 in motif IV and G136 in motif V can be partly attributed to their defect in metal cofactor coordination. Alanine substitution at amino acid 118 primarily reduces the level of binding to the nicked product, suggesting that R118 plays a significant role in postcleavage DNA−protein interaction. Binding and cleavage analyses of multiple mutants at positions Y80 and H116 underscore the role these residues play in protein−DNA interaction and implicate their potential involvement as a hydrogen bond donor in recognition of deaminated DNA bases. DNA cleavage analysis using mutants defective in DNA binding reveals a novel 3′-exonuclease activity in endonuclease V. An alternative model is proposed that entails lesion specific cleavage and endonuclease to 3′-exonuclease mode switch by endonuclease V for removal of deaminated base lesions during endonuclease V-mediated repair.

Endonuclease V is a DNA repair enzyme that repairs deaminated base damage by hydrolyzing the second phosphodiester bond 3′ from a base lesion (*1*, *2*). All deaminated lesions, including deoxyinosine, deoxyxanthosine, deoxyoxanosine, and deoxyuridine, are substrates for endonuclease V; albeit, the catalytic efficiencies vary significantly (*1*−*10*). The involvement of *Escherichia coli* endonuclease V in repair of deamination DNA base lesions and N^6-hydroxylaminopurine has been substantiated by genetic studies (*11*−*13*). One of the biochemical properties revealed by binding and kinetic analyses is the ability of the enzyme to remain bound to nicked deaminated lesions after strand cleavage (*2*, *6*). As in other DNA repair glycosylases such as MutY and human TDG (*14*, *15*), this unique property may act as a sensor for recruitment of other proteins for a downstream repair process (*2*).

Given that endonuclease V is a ubiquitous protein in nature, with its homologues found in eubacteria, archaea, and eukaryotes, it is essential that the structure−function relationship of this repair enzyme be understood. In this respect, endonuclease V from the thermophilic bacterium *Thermotoga maritima* (Tma)[1] provides an ideal model system since the protein is thermostable and easily amenable to site-directed mutagenesis analysis. Previous site-directed mutagenesis analysis reveals three highly conserved amino acid residues involved in metal cofactor coordination and catalytic function (*16*). Tyrosine at position 80 was shown to play a role in substrate and product binding. An alanine substitution at Y80 resulted in a reduced level of binding and multiple turnovers (*16*).

The vast amount of progress made in genome sequencing of many organisms allows for identification of evolutionarily conserved amino acid residues by sequence alignment. Taking advantage of the thermostable Tma endo V system, we conducted a systematic site-directed mutagenesis analysis on all seven conserved regions defined as motifs I−VII (Figure 1). The DNA cleavage activities of all mutants were examined using inosine-, xanthosine-, oxanosine-, and uridine-containing double-stranded and single-stranded DNA. Mutants that exhibited significantly different activities were investigated by gel mobility shift assays using the inosine-containing DNA substrate and the nicked inosine product to determine their binding affinity for both the substrate and product. Mutants affecting binding were subject to kinetic analysis for characterization of their effect on enzymatic turnover. These detailed analyses define a series of important

† This work was supported in part by CSREES/USDA (SC-1700274, Technical Contribution 5092), the National Institutes of Health (Grant GM 067744), the Concern Foundation, and Howard Hughes Medical Institute Undergraduate Fellowships.

* To whom correspondence should be addressed. E-mail: wgc@clemson.edu. Telephone: (864) 656-4176. Fax: (864) 656-0393.

[1] Abbreviations: BSA, bovine serum albumin; dNTP, deoxyribonucleoside triphosphate; DTT, dithiothreitol; 6-Fam, 6-carboxyfluorescein; endo V, endonuclease V; HEPES, *N*-(2-hydroxyethyl)piperazine-*N*′-2-ethanesulfonic acid; I, deoxyinosine; PAGE, polyacrylamide gel electrophoresis; PCR, polymerase chain reaction; Tma, *Thermotoga maritima*; U, deoxyuridine; wt, wild-type; X, deoxyxanthosine.

10.1021/bi050837c CCC: $30.25 © 2005 American Chemical Society
Published on Web 08/06/2005

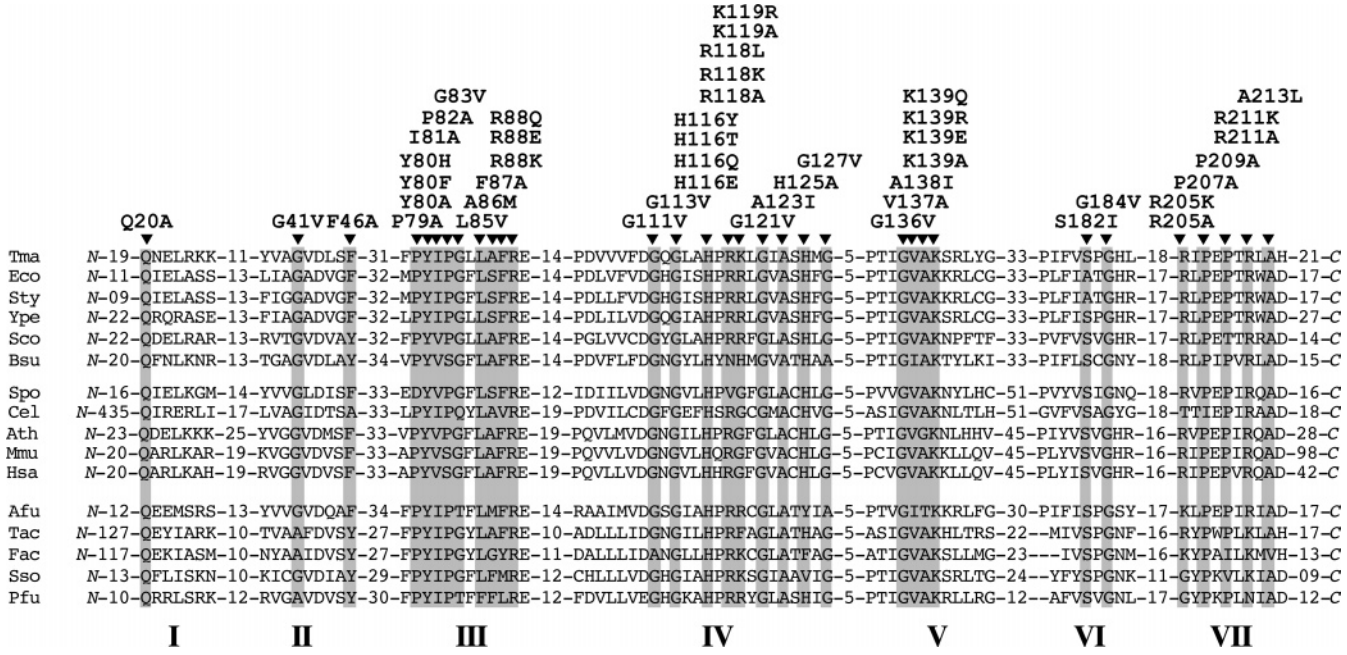

FIGURE 1: Sequence alignment of endonuclease V. Amino acid residues selected for site-directed mutagenesis are highlighted, and the resulting mutants are indicated above the arrows. GenBank accession numbers are shown after the species names: Tma, *T. maritima*, NP_229661; Eco, *E. coli*, NP_418426; Sty, *Salmonella typhimurium*, NP_463037; Ype, *Yersinia pestis*, NP_667835; Sco, *Streptomyces coelicolor*, CAB40676; Bsu, *Bacillus subtilis*, BSUB0019; Spo, *Schizosaccharomyces pombe*, 1723511; Cel, *Caenorhabditis elegans*, 1731299; Ath, *Arabidopsis thaliana*, T10669; Mmu, *Mus musculus*, XP_203558; Hsa, *Homo sapiens*, BAC04765; Afu, *Archaeoglobus fulgidus*, NP_068968; Tac, *Thermoplasma acidophilum*, CAC11602; Fac, *Ferroplasma acidarmanus*, ZP_00001774; Sso, *Sulfolobus solfataricus*, NP_343804; and Pfu, *Pyrococcus furiosus*, NP_578716.

amino acid residues interacting with DNA and affecting enzymatic turnover. Using mutants with a reduced level of DNA binding, this work revealed 3′-exonuclease activity by endonuclease V. A potential role of the 3′-exonuclease activity in endonuclease V-mediated deaminated repair processing is discussed.

EXPERIMENTAL PROCEDURES

Reagents, Media, and Strains. All routine chemical reagents were purchased from Sigma Chemicals (St. Louis, MO), Fisher Scientific (Suwanee, GA), or VWR (Suwanee, GA). Restriction enzymes and T4 DNA ligase were purchased from New England Biolabs (Beverly, MA). DNA sequencing kits were purchased from Applied Biosystems (Foster City, CA). BSA and dNTPs were purchased from Promega (Madison, WI). *Taq* DNA polymerase was purchased from Eppendorf (Hamburg, Germany). Deoxyoligonucleotides were ordered from Integrated DNA Technologies Inc. (Coralville, IA). LB medium was prepared according to standard recipes. GeneScan Stop Buffer consisted of 80% formamide (Amresco, Solon, OH), 50 mM EDTA (pH 8.0), and 1% blue dextran (Sigma Chemicals). TB buffer (1×) consisted of 89 mM Tris base and 89 mM boric acid. TE buffer consisted of 10 mM Tris-HCl (pH 8.0) and 1 mM EDTA. *E. coli* host strain AK53 (*mrr*B$^-$, MM294) was from our laboratory collection.

Site-Directed Mutagenesis of Tma Endo V. An overlapping extension PCR procedure was used for site-directed mutagenesis (*17*). PCR products digested with a pair of *Nde*I and *Bam*HI endonucleases were ligated to cloning vector pEV5 treated with the same pair of restriction endonucleases. The ligated vectors were transformed into *E. coli* strain AK53 (*mrr*B$^-$, MM294). Plasmids containing inserts were reisolated and sequenced on an ABI sequencer using dye-dideoxy terminator chemistry to identify mutated sequence and ensure that the constructs were free of PCR error. An overnight *E. coli* AK53 LB culture containing the desired site-directed mutation was diluted 100-fold into MOPS medium supplemented with 50 μg/mL ampicillin. The *E. coli* cells (1 L) were grown at 37 °C while being shaken at 250 rpm overnight. The cells were collected by centrifugation at 4000 rpm and 4 °C, washed once with precooled PBS buffer, and stored at −20 °C. Protein purification and quantitation were carried out essentially as previously described (*2*, *16*).

Oligonucleotide Substrates. The sequences of the oligonucleotides are shown in Figure 2A. Oligonucleotides containing inosine or uridine were ordered from IDT and purified by PAGE. The oligonucleotides were dissolved in TE buffer at a final concentration of 10 μM. The two complementary strands with the unlabeled strand in 1.2-fold molar excess were mixed, incubated at 85 °C for 3 min, and allowed to form duplex DNA substrates at room temperature for more than 30 min. Oligonucleotides containing xanthosine (X) or oxanosine (O) were prepared as previously described (*18*).

Tma Endo V Cleavage Assays. The cleavage reaction mixtures (10 μL) containing 10 mM HEPES-KOH (pH 7.4), 1 mM DTT, 2% glycerol, 5 mM $MgCl_2$ (unless otherwise specified), 10 nM oligonucleotide DNA substrate, and 100 nM Tma endo V protein unless otherwise specified were incubated at 65 °C for 30 min. The reactions were terminated by addition of an equal volume of GeneScan Stop Buffer. The reaction mixtures were then heated at 94 °C for 3 min and cooled on ice. Samples (3.5 μL) were loaded onto a 10% denaturing polyacrylamide gel containing 7 M urea. Electrophoresis was conducted at 1500 V for 1.6 h using an ABI

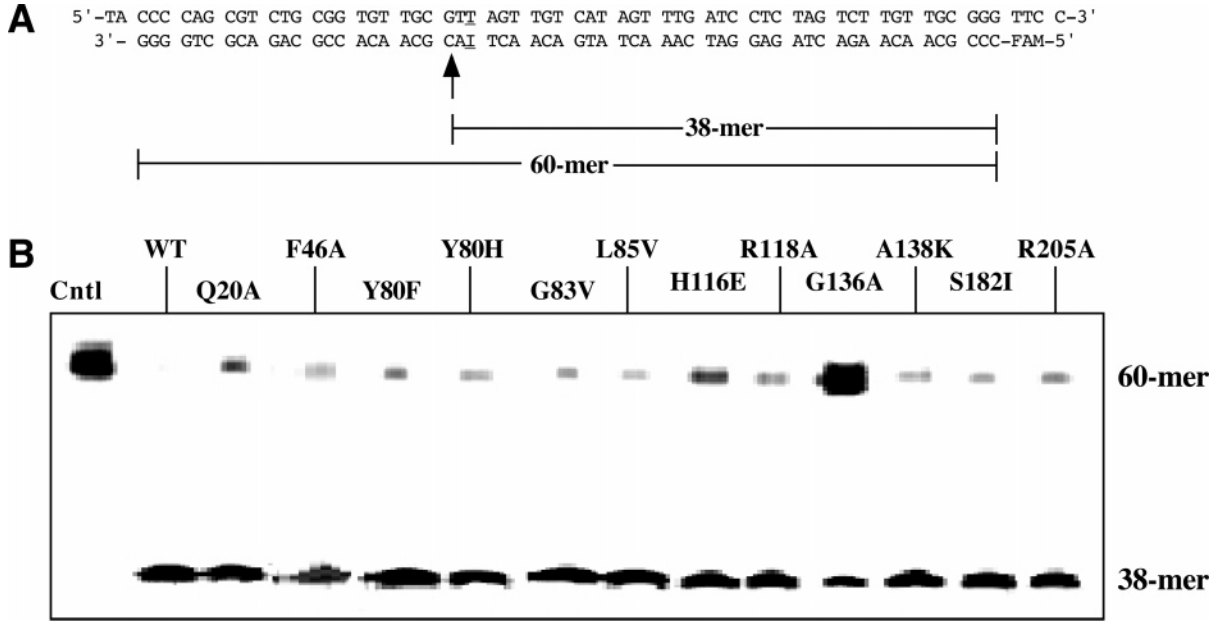

FIGURE 2: DNA cleavage assay of Tma endonuclease V. (A) Lesion-containing oligonucleotide substrate. The 5′ end of the bottom strand was labeled with the Fam fluorophore. (B) Cleavage activity of wt and mutant Tma endo V on inosine-containing substrate (T/I). Cleavage reactions were performed as described in Experimental Procedures with 100 nM wt or mutant Tma endo V protein.

377 sequencer (Applied Biosystems). Cleavage products and remaining substrates were quantified using GeneScan analysis software version 3.0.

Gel Mobility Shift Assays. The binding reaction mixtures (20 μL) contained 100 nM fluorescently labeled oligonucleotide DNA substrates, 5 mM $CaCl_2$ or 5 mM EDTA, 20% glycerol, 10 mM HEPES-KOH (pH 7.4), 1 mM DTT, and the indicated amount of Tma endo V protein. The binding reactions were carried out at 65 °C for 30 min. Samples were electrophoresed on a 6% native polyacrylamide gel in 1× TB buffer supplemented with 5 mM $CaCl_2$ or EDTA. The bound and free DNA species were analyzed using a Typhoon 9400 Imager (Amersham Biosciences) with the following settings: PMT at 600 V, excitation at 495 nm, and emission at 535 nm.

RESULTS

Motifs in Endonuclease V. Endonuclease V is a conserved DNA repair protein ubiquitously found in nature. The prokaryotic homologues of endonuclease V family proteins are around 200 amino acids in length, while the mammalian homologues are around 300 amino acids in length. Our understanding of the structure−function relationship of this repair enzyme's substrate specificity is limited. To initiate a systematic site-directed mutagenesis study to define the functional role of important amino acid residues, we aligned endo V homologues from eubacteria, archaea, and eukaryotic organisms using the CLUSTAL method (*19*). This sequence alignment allowed us to identify seven conserved regions universal to all endonuclease V family proteins (Figure 1). The spacing between motifs is well-conserved except that between motifs V and VI, which is shortest in archaea, intermediate in eubacteria, and longest in eukaryotes. The mammalian homologues also contain additional residues at the C-termini (Figure 1). Some endo V family proteins such as the one from *Caenorhabditis elegans* have additional domains at the N-termini. The three conserved active site residues identified by previous biochemical analysis are located as D43 in motif II, E89 in motif III, and D110 in motif IV (Figure 1, numbering based on the Tma endo V sequence) (*16*).

Site-Directed Mutagenesis of Tma Endonuclease V. To delineate a detailed structure−function map of the endo V proteins, we made 47 site-directed mutants at 32 sites encompassing all seven motifs. At many sites, multiple mutations were introduced to comprehensively probe the effects of amino acid substitutions on enzymatic function (Figure 1). To characterize these mutants, we assayed DNA cleavage activity using double-stranded and single-stranded deaminated base-containing substrate (Figure 2A). The 60-mer bottom strand was fluorescently labeled with FAM (6-carboxyfluorescein). An endo V-mediated cleavage event generates a 38-mer that can be visualized on a GeneScan gel (Applied Biosystems). A representative gel is shown in Figure 2B, and the complete data set is summarized in Table 1. The initial DNA cleavage assay was performed with the enzyme in excess to reveal any low-level enzyme activity.

Motifs I and II. Motif I contains an invariant Gln residue. Substitution of Q20 with Ala had no effect on inosine or xanthine cleavage for either double- or single-stranded DNA, while the extent of cleavage of oxanosine or uridine was reduced to <50% (Table 1). Motif II includes the active site D43 residue that is essential for catalysis (Figure 1) (*16*). G41V and F46A mutations reduced the levels of oxanosine and uridine cleavage to <40%. The effect on cleavage of the single-stranded uridine substrate appeared to be more significant than that for the double-stranded uridine substrate (Table 1). However, the cleavage of inosine and xanthosine substrates was not affected.

Motif III. Thirteen mutations were introduced at nine sites in motif III, which contains the catalytic residue E89 (Figure 1) (*16*). Mutations at the four conserved residues, P79A, F87A, I81A, and P82A, essentially maintained wild-type level activity toward inosine, xanthosine, oxanosine, and

Table 1: Percent Cleavage of Inosine-, Xanthosine-, Oxanosine-, and Uridine-Containing DNA[a]

		inosine		xanthosine		oxanosine		uridine	
motif	endo V	T/I	ss I	T/X	ss X	T/O	ss O	G/U	ss U
	wt	100	100	100	100	100	100	100	100
I	Q20A	84	99	98	96	30	29	36	41
II	G41V	98	96	91	97	20	12	40	14
	F46A	98	98	95	97	18	14	27	5
III	Y80A	92	98	97	97	7	7	3	0
	Y80F	94	99	97	96	11	11	35	10
	Y80H	94	99	98	97	9	9	9	0
	G83V	95	100	96	96	10	0	15	0
	L85V	95	100	97	96	10	11	7	0
	A86M	101	100	97	97	14	12	19	5
	R88E	95	99	97	100	24	21	40	13
	R88K	100	99	97	99	45	30	80	30
	R88Q	88	98	98	96	13	13	16	5
IV	G111V[b]	57	82	89	96	0	7	0	2
	G113V	57	98	91	96	6	9	3	0
	H116E	80	99	100	96	0	7	4	1
	H116Q	98	100	100	96	8	22	55	31
	H116T	97	100	95	95	56	46	101	61
	H116Y	92	99	93	94	0	8	10	3
	R118A	102	99	100	100	57	54	52	55
	R118K	96	81	100	100	5	2	4	1
	R118L[b]	92	96	99	96	25	10	10	5
	K119A[b]	110	99	100	94	57	23	36	20
	K119R	95	98	100	100	33	33	36	26
	G121V	82	97	96	96	8	7	2	6
	A123I	93	100	103	95	5	7	3	5
	G127V[b]	28	94	94	89	6	5	1	1
V	G136V	34	28	38	44	5	8	1	1
	V137A	89	93	96	98	5	9	4	1
	A138I	91	99	91	97	10	8	9	6
	K139A	90	100	92	95	6	8	2	0
	K139E	99	101	93	93	0	6	0	7
	K139R	89	100	92	94	0	0	2	0
	K139Q	89	99	91	97	6	0	6	5
VI	S182I	83	100	91	96	7	15	9	10
	G184V[b]	86	66	81	77	6	14	5	0
VII	R205A	94	100	101	96	10	26	8	22
	R205K	97	101	95	97	94	111	96	83
	P207A	94	103	91	95	56	57	51	17
	P209A	96	101	96	97	85	94	107	94
	R211A	85	101	95	95	61	51	42	46
	R211K	95	101	93	98	41	37	55	35
	A213L[b]	40	34	69	75	9	4	1	4

[a] The reactions were performed with 100 nM endo V, 10 nM substrate, and 5 mM $MgCl_2$. [b] The reactions were performed with 10 nM endo V, 10 nM substrate, and 5 mM $MgCl_2$ due to relatively low-level protein expression. Comparisons were made with the wt enzyme assayed under the same condition.

uridine substrates except that I81A and P82A were ~40 and ~70% less active, respectively, toward oxanosine substrates (data not shown). Previous studies have shown that the Y80A substitution essentially abolishes cleavage of uridine substrates while maintaining inosine cleavage (*16*). Results from this work were consistent with previous conclusions and showed that Y80A, Y80F, and Y80H were still fully active toward inosine and xanthosine substrates, but were minimally active on oxanosine and uridine substrates, except that Y80F was partially active on the G/U substrate (Table 1). The ability of Y80F to maintain considerable cleavage activity on the G/U substrate indicates that the benzene side chain in Y80F plays a functional role in endo V. G83V, L85V, A86M, R88E, and R88Q were catalytically similar in that they were fully active on inosine and xanthosine substrates but experienced significant loss in the levels of oxanosine and uridine cleavage (Table 1). The positive charge at R88 obviously was important since the oxanosine and uridine cleavage by R88K was more significant than those of other mutants such as R88Q. This is consistent with the sequence alignment showing R88 as an invariant residue next to the catalytic E89 residue in motif III (Figure 1).

Motif IV. Fifteen amino acid substitutions were analyzed at nine positions in motif IV (Figure 1). This motif contains five invariant or highly conserved small amino acids (G111, G113, G121, A123, and G127). G111V, G113V, G121V, A123I, and G127V exhibited levels of oxanosine and uridine cleavage of less than 10% (Table 1). G111V, G113V, G121V, and G127V substitutions reduced the level of cleavage of the T/I substrate by ~40, ~50, ~10, and ~70%, respectively (Table 1). At H116, the reduction in the level of oxanosine and uridine cleavage followed this order: H116T < H116Q < H116Y < H116E (Table 1). H116E also caused a small reduction in the level of T/I cleavage (Table 1). Substitutions at R118 and K119 primarily affected oxanoine and uridine cleavage, and the effect did not appear to be dependent on the positive charge since the R118K and K119R mutants were not more active than other substitutions (Table 1). Consistent with the previous study (*16*), H125A had significant activities on all substrates (data not shown).

Motif V. This motif contains a highly conserved GVAK sequence (Figure 1). The invariant G136 seemed to be critical for cleavage since this was the first time we observed an amino acid substitution that affected cleavage of all eight substrates substantially (Table 1). The effects of substitutions at V137, A138, and K139 were primarily on oxanosine and uridine cleavage; however, V137A, A138I, K139A, K139R, and K139Q reduced the level of T/I cleavage by ~10% (Table 1).

Motif VI. This motif contains the highly conserved S182 and the invariant G184 (Figure 1). In addition to the substantial reduction in the level of oxanosine and uridine cleavage, S182I and in particular G184V reduced the level of inosine and xanthosine cleavage (Table 1).

Motif VII. Among the seven mutations introduced into motif VII, P207A, P209A, R211A, and R211K still maintained significant activities toward all substrates (Table 1). The positive charge at R205 seemed to be important in oxanosine and uridine cleavage since R205K but not R205A exhibited wt activity (Table 1). Substitution of A213 with a bulkier Leu resulted in significant reduction not only in the level of cleavage of oxanosine and uridine substrates but also in the level of cleavage of inosine and uridine substrates (Table 1).

Binding to the T/I Substrate. To discern the effects of site-directed mutations on binding, we conducted gel mobility shift analysis using the T/I substrate on all mutants except a few in which the proteins were expressed at a low level. The mutants that exhibited a significant effect on binding are shown in Figure 3. Q20A in motif I reduced the level of binding by more than 50%. Elimination of the hydroxyl group of Y80 in motif III amounted to an ~40% reduction in binding affinity (Figure 3). Y80H, as a result of substitution of the benzene ring with the imidazole side chain, maintained only ~10% binding affinity. Complete elimination of the aromatic ring as shown by Y80A rendered the binding undetectable by the gel mobility shift assay. G83V

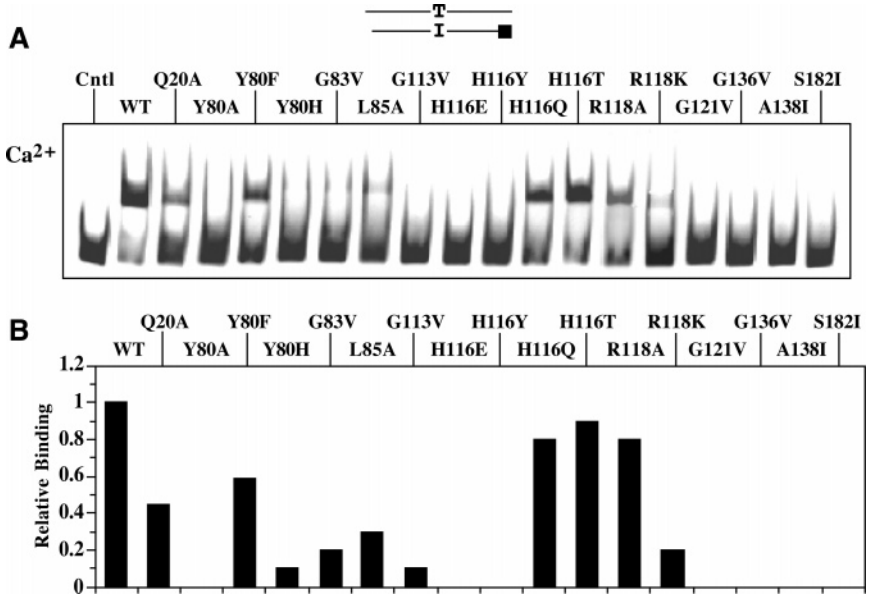

FIGURE 3: Binding analysis of Tma endo V mutants on double-stranded inosine-containing DNA substrate. (A) Gel mobility shift analysis of binding of Tma endo V to double-stranded inosine-containing substrate (T/I) with 5 mM $CaCl_2$. Gel mobility shift assays were performed as described in Experimental Procedures with 100 nM endo V protein, 100 nM T/I substrate, and 5 mM $CaCl_2$. (B) Quantitative analysis of the binding affinity of Tma endo V matants for the T/I substrate. The binding affinity of wt Tma endo V was taken to be 1.0.

and L85A substitutions in motif III also reduced the the level of binding to below 20% (Figure 3). Two Gly residues in motif IV appeared to be important for binding since G113V and G121V showed little binding affinity for the T/I substrate (Figure 3). The binding effect of H116 substitutions followed this order: H116T < H116Q < H116Y and H116E [a trend consistent with the initial cleavage analysis of the T/I substrate (Table 1)]. The R118K mutant showed less affinity than the R118A mutant, in keeping with the cleavage analysis demonstrating that the positively charged Lys cannot substitute for the Arg at this position. Mutations at G136 and A138 in motif V had a profound effect on binding as evidenced by the lack of retarded bands in G136V and A138I mutant lanes (Figure 3). Bulkier and hydrophobic residues at position 182 in motif VI did not seem to be favored as the S182I mutant did not show any observable binding by gel mobility shift analysis. In motif VII, all the mutants that were analyzed, including R205A, R205K, P207A, P209A, R211A, and R211K, showed wt level binding (data not shown). A213L was not assayed because of a relatively low level of protein expression.

Kinetic Analysis of T/I Cleavage. To test the effect that these 17 mutants had on enzymatic turnover, we performed kinetic analysis under the condition that the substrate was in 10-fold excess ([E]:[S] ratio = 1:10) (Figure 4). Previous studies have already showed that wt Tma endo V only achieves very limited turnover under the same reaction conditions (*2*). The kinetic behavior of Q20A in motif I was similar to that of the wt enzyme, demonstrating only limited turnover (data not shown). Among the three Y80 mutants, only Y80F exhibited limited turnover. Y80H and Y80A were able to achieve multiple turnover (Figure 4A), a pattern consistent with the binding data (Figure 3). As expected from the low binding affinities, G83V and L85A in motif III turned over the T/I substrate multiple times to essentially complete the reaction (Figure 4A). Mutants in motif IV fall into three categories. First, the T/I cleavage by G113V over the entire time course was limited (Figure 4B), suggesting that this mutant was catalytically not as active as the wt enzyme. Second, H116T and H116Q appeared to behave like the wt enzyme (Figure 4A,B). Third, the two low-binding affinity mutants, H116E and H116Y, showed multiple turnovers (Figure 4B). All three mutants in motif IV (R118A, R118K, and G121V) also were able to turn over the T/I substrate (Figure 4C). Like G113V in motif IV, G136V in motif V appeared to have a low catalytic activity, which resulted in limited cleavage (Figure 4D). The low-binding affinity mutant A138I showed multiple turnovers (Figure 4D). S182I was able to turn over the T/I substrate, but to an extent that was less than that of A138I (Figure 4D). To determine whether the reaction catalyzed by S182I had simply reached a plateau or was slower than that by G136V, we extended the incubation time to 240 min. Indeed, the T/I cleavage reached 85% completion after 240 min (data not shown), indicating that the S182I mutant is catalytically slower than other multiple-turnover mutants.

Binding to the Nicked T/I Product. To determine whether the ability to turnover the T/I substrate was due to weakened binding to the nicked T/I product, we assessed the binding by gel mobility shift. All mutants that were able to turn over the T/I substrate showed less than 50% binding affinity for the nicked T/I product as compared with the wt enzyme (Figure 5, Y80A, Y80H, G83V, L85A, G113V, H116E, H116Y, R118A, R118K, G121V, G121V, G136V, A138I, and S182I). Other mutants that maintained at least 50% binding affinity showed only limited turnover (Figure 5, Q20A, Y80F, H116Q, and H116T). These results indicate that indeed the enzymatic turnover is closely related to the binding affinity of the enzyme for the nicked T/I product. The binding affinity of these mutants to the nicked T/I product is in the same order as that for the T/I substrate except for R118A (Figures 3 and 5). Thus, mutations at these sites in general affect both substrate and product binding. However, Ala substitution at R118 seems to primarily affect product binding (Figure 5).

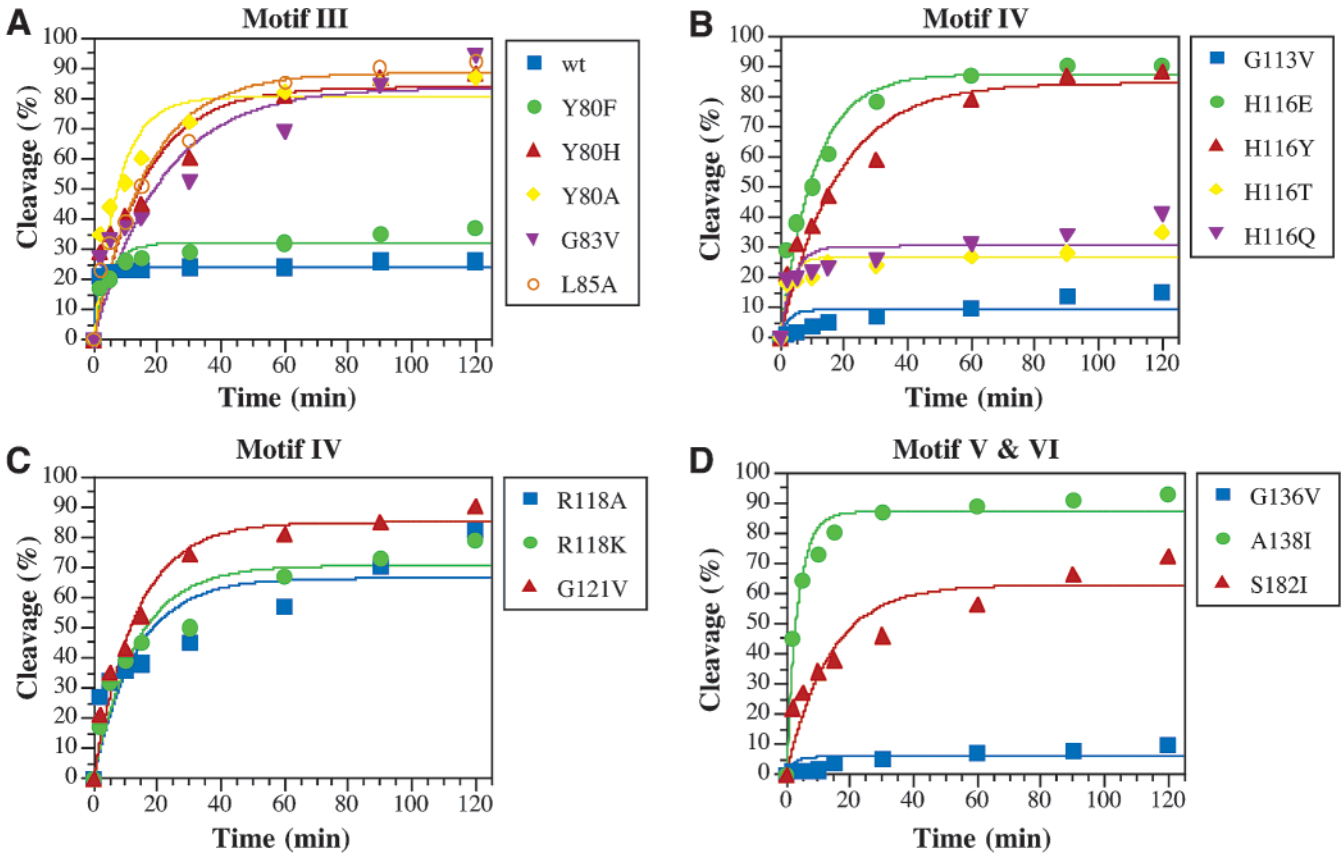

FIGURE 4: Time course analysis of T/I cleavage by wt and mutant Tma endo V. Cleavage reactions were performed as described in Experimental Procedures with 1 nM Tma endo V ([E]:[S] ratio = 1:10). Reactions were stopped on ice at the indicated time points, followed by addition of an equal volume of GeneScan Stop Buffer. (A) Quantitative analysis of T/I cleavage by mutants in motif III. (B) Quantitative analysis of T/I cleavage by mutants in motif IV. (C) Quantitative analysis of T/I cleavage by mutants in motif IV. (D) Quantitative analysis of T/I cleavage by mutants in motif V and VI.

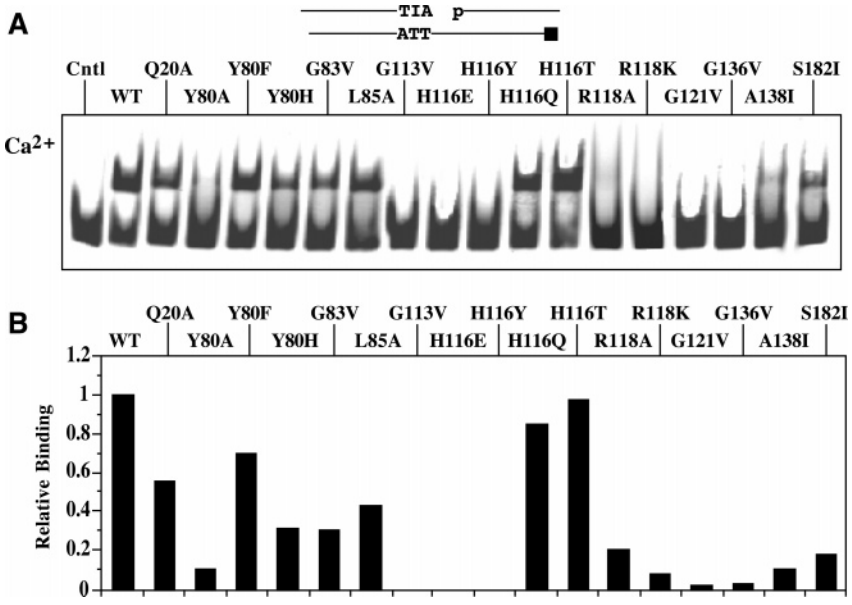

FIGURE 5: Binding analysis of Tma endo V mutants on the double-stranded nicked inosine-containing DNA substrate. (A) Gel mobility shift analysis of binding of Tma endo V to the double-stranded nicked inosine-containing substrate (I/T) with 5 mM $CaCl_2$. Gel mobility shift assays were performed as described in Experimental Procedures with 100 nM endo V protein, 100 nM nicked I/T substrate, and 5 mM $CaCl_2$. The nicked I/T substrate contains inosine at the penultimate position of the upstream top strand as previously described (*2*). (B) Quantitative analysis of the binding affinity of Tma endo V mutants for the T/I substrate. The binding affinity of wt Tma endo V was taken to be 1.0.

Affinities of G113V and G136V for Mg^{2+}. G113V in motif IV and G136V in motif V showed low cleavage activity compared with the wt enzyme in the time course analysis, suggesting that catalysis of DNA cleavage may have been affected (Figure 4). Since endo V is a metal-dependent enzyme, one possible reason for the low activity is that these mutants may somehow disturb metal coordination. To test this possibility, we examined the effect of Mg^{2+} concentra-

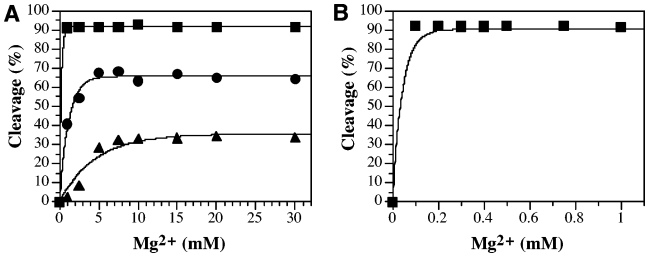

FIGURE 6: Effect of Mg^{2+} concentration on DNA cleavage by G113V and G136V. Cleavage reactions were performed as described in Experimental Procedures. (A) Mg^{2+} titration with 0−30 mM $MgCl_2$: (■) wt Tma endo V, (●) G113V, and (▲) G136V. (B) Mg^{2+} titration with 0−1 mM $MgCl_2$: (■) wt Tma endo V.

tion on DNA cleavage (Figure 6A). For the wt enzyme, addition of 1 mM Mg^{2+} appeared to be sufficient to support full DNA cleavage activity, suggesting that wt endo V possesses a high affinity for the metal cofactor. G113V and G136V required high Mg^{2+} concentrations to reach maximal activity. The apparent K_d values of G113V and G136V for Mg^{2+} were estimated to be 0.6 and 3.6 mM, respectively. The tight binding of the wt enzyme to the Mg^{2+} was further verified by titrating Mg^{2+} at lower concentrations (Figure 6B). Close to complete DNA cleavage was observed with a Mg^{2+} concentration as low as 0.1 mM, suggesting that the apparent K_d value of the wt enzyme for Mg^{2+} was below 0.1 mM. Thus, G113V and G136V mutations reduced the binding affinity for Mg^{2+} at least 6- and 36-fold, respectively. High Mg^{2+} concentrations, however, did not seem to fully rescue the cleavage activity (Figure 6A), suggesting that G113V and G136V may cause other defects in addition to metal cofactor binding.

3′-Exonuclease Activity in Endonuclease V. In our previous studies, we detected some nonspecific nuclease activity when Mn^{2+} was used as the metal cofactor (*9*). However, due to fewer nonspecific cleavage bands, which were also too close to the end of migration, it was difficult to make a good judgment about whether they are caused by 3′-exonuclease activity or other nuclease activity. We reasoned that mutants with reduced DNA binding may have a more profound effect on the processivity of nonspecific nuclease activity and, therefore, reveal its enzymatic nature. With the exception of G113V, H116Y, G121V, and G136V, the majority of the binding defective mutants indeed exhibited an extended ladder as compared with the wt enzyme (Figure 7). Since the bottom cleavage strand was labeled with 5′-Fam, such a ladder is a clear indication of 3′-exonuclease activity in endonuclease V. The wt enzyme is likely more processive, resulting in more complete 3′-exonuclease degradation. However, the reduced processivity of these mutants may cause more frequent dissociation, resulting in a distinct ladder. Judging from the spacing of the ladder, we roughly estimated that most of the mutants start to dissociate from the specific cleavage product (38-mer) after six 3′-exonuclease cleavage events. Remarkably, all the 3′-exonuclease cleavage products were smaller than the specific inosine cleavage product (38-mer). Given that some mutants such as G83V and K119R still had a significant amount of uncleaved T/I substrate, one would imagine that one should have observed some ladder between the 60-mer substrate and the 38-mer specific cleavage product if the 3′-exonuclease activity could be initiated from the very 3′ end. Yet, we have not observed such a laddering pattern. This result indicates that the 3′-exonuclease activity might be preferentially triggered by the specific cleavage event at the inosine site.

DISCUSSION

Endonuclease V is a relatively small but ubiquitous protein found in eubacteria, archaea, and eukarotic organisms, including mammals. Biochemical and genetic analyses in *E. coli* demonstrate its involvement in deamination repair of inosine and xanthosine lesions (*1*, *7*, *11*, *12*). The sequence elements involved in DNA−protein interactions in general and deaminated lesion recognition in particular are not well defined. This work takes a systematic site-directed mutagenesis approach to mapping the conserved amino acid residues that are involved in DNA−protein interactions. Taking advantage of binding defective mutants, this study reveals a novel 3′-exonuclease activity in endonuclease V.

DNA−Protein Interactions and Conserved Motifs. Seven conserved motifs have been identified from sequence alignment of endonuclease V family proteins from eubacteria, eukaryotes, and archaea (Figure 1). D43 in motif II, E89 in motif III, and D110 in motif IV are active site residues involved in coordination of catalytic metal ions (Figure 8A) (*16*). Q20A in motif I, as an invariant residue, has a moderate effect on both substrate and product binding (Figures 3 and 5), the extent of which does not seem sufficient to cause a significant increase in the level of enzymatic turnover. Motif I bears some similarity to the QXXL motif, which was previously identified as a clamp binding motif (*20*). Some of the *E. coli* proteins bearing this motif indeed interact with the β clamp of the DNA polymerase holoenzyme (*21*). We have tested this possibility using the protein shift assay or gel mobility shift assay, but thus far have not found such an interaction (F. J. Lopez de Saro, H. Gao, W. Cao, and M. O'Donnell, unpublished observation). However, this does not preclude the possibility that they may interact in the presence of additional protein(s).

Motifs III−VI contain many residues that directly or indirectly affect DNA−protein interactions (Figure 8A). Y80, G83, and L85 in motif III, G113, H116, and G121 in motif IV, G136 and A138 in motif V, and S182 in motif VI have a profound effect on both substrate and product binding (Figures 3 and 5). The significantly reduced level of binding was corroborated by the kinetic analysis, which assessed the enzymatic turnover using the T/I substrate (Figure 4). Substitution of the invariant Y80 with multiple amino acids dissects roles of different side chains in binding. Evidently, from the comparison of the wt enzyme (Y80) and Y80F, the hydroxyl group plays a role in binding (Figures 3 and 5). The aromatic side chain is important for both substrate and product binding since the loss of the ring has a profound effect on binding (Y80A) (Figure 3 and ref *16*). Results obtained from analysis of Y80H indicate that the aromatic phenol ring cannot be substituted with the aromatic imidazole ring. The four substitutions at H116 are also illuminating (Figures 3−5). H116Q and H116T, both of which have the hydrogen bond-donating side chain, maintain close to wt level binding, whereas H116E does not. The imidazole ring in H116 apparently cannot be substituted with a phenol ring as seen in H116Y. The effect caused by the R118A

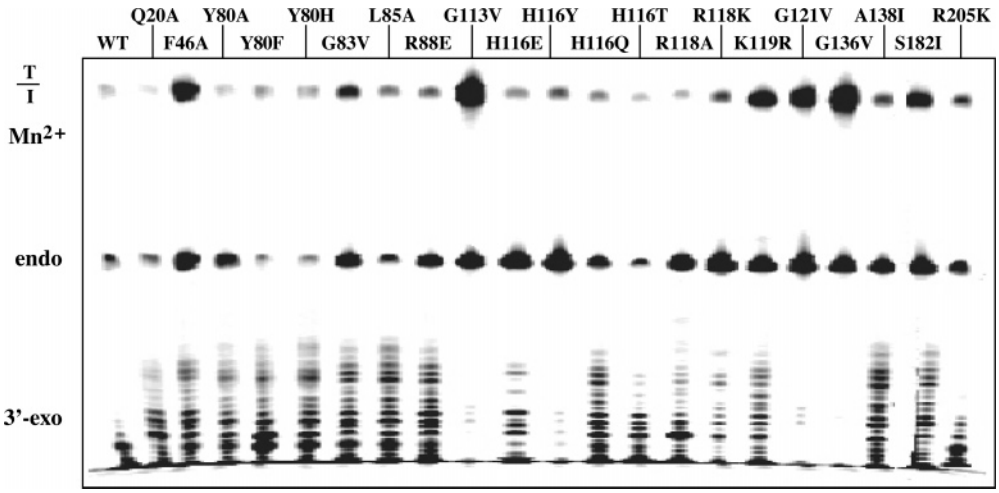

FIGURE 7: 3′-Exonuclease activity of Tma endo V mutants on the T/I substrate. Cleavage reactions were performed as described in Experimental Procedures with 5 mM $MnCl_2$.

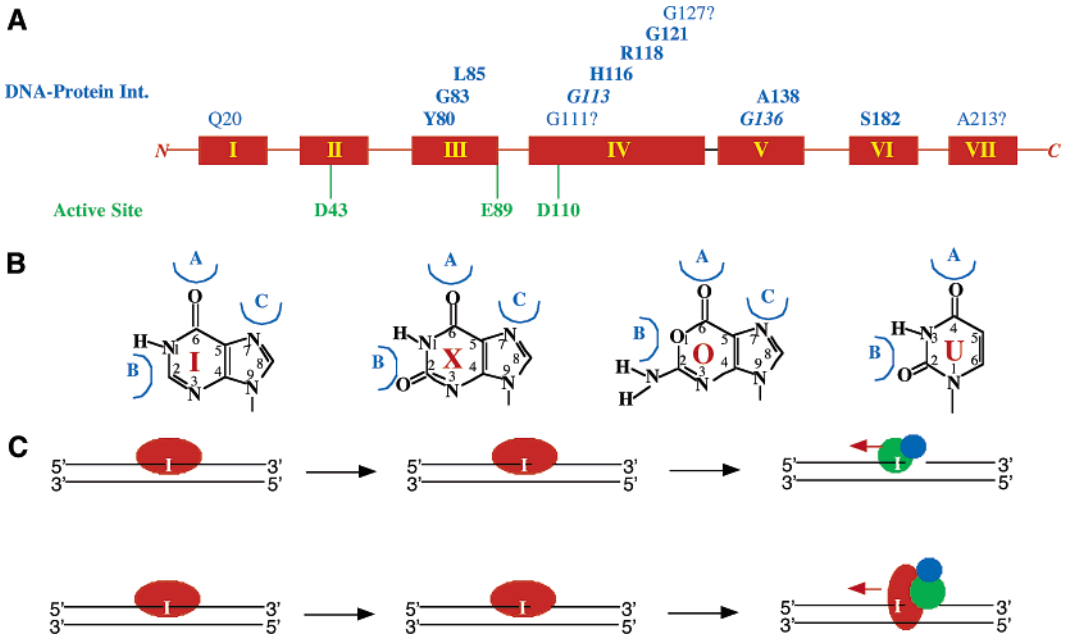

FIGURE 8: DNA−protein interactions and switch of mode model for endonuclease V-mediated repair. (A) Conserved motifs and DNA−protein interactions. Residues that significantly affect DNA binding are bold. Residues that have low catalytic activity are italic. Residues that may affect binding but were not studied due to low-level protein expression are followed by a question mark. (B) A hypothetical model of deaminated base recognition. Elements A−C are putative recognition elements in endonuclease V. I represents deoxyinosine, X deoxyxanthosine, O deoxyoxanosine, and U deoxyuridine. (C) Proposed models for endonuclease V-mediated repair. I represents deoxyinosine. The ovals represent endo V and the circles putative endo V-interacting proteins. After the inosine strand is nicked, the model shown at the top suggests that endo V is displaced by downstream protein(s) from the lesion and a 3′-exonuclease other than endo V initiates the removal of the deaminated lesion from DNA (*5*, *7*, *13*). An alternative model shown at the bottom based on data obtained from this study illustrates that endo V recruits other protein(s) to the repair site, which switch endo V from endonuclease mode to 3′-exonuclease mode for removal of the deaminated lesion from DNA.

substitution mainly occurs at the product binding step, which resulted in multiple turnovers despite the strong binding to the substrate (Figures 3−5). G113 and G136 not only affect the binding but also reduce the rate of catalysis substantially as demonstrated by the kinetic analysis (Figure 4). The defect in catalysis can be explained in part by the reduced binding affinity for Mg^{2+} (Figure 6). Mutations at G113 or G136 may indirectly alter the metal binding pocket, or alternatively, these two Gly residues may be involved in metal binding directly through the backbone carbonyl group. G111V and G127V in motif IV, G184V in motif VI, and A213L in motif VII are substitutions that affect cleavage of all four deaminated lesions; however, the low level of protein expression precludes binding analysis in this study. Placing a small amino acid residue such as Gly or Ala at these positions may be important for the structural integrity of the endonuclease V protein.

Conserved Residues and Base Recognition. A general trend that emerged from this work is that mutants often maintain inosine and xanthosine cleavage but reduce or eliminate oxanosine and uridine cleavage (Table 1). This trend raises the question of why oxanosine cleavage and uridine cleavage are particularly vulnerable to amino acid substitutions and how this vulnerability is related to the deaminated base recognition mechanism. Previously, we proposed a three-element base recognition mechanism to

account for the ability of endonuclease V to recognize all four deaminated bases (Figure 8B and ref *9*), which posits that elements A and C recognize the 6-keto (or 4-keto in uracil) and the N^7 position of a purine base. Element B is snug between the N^1 and C^2 positions in inosine and xanthosine, or the equivalent position in oxanosine or uridine. This model, though hypothetical, may explain the different effects on cleavage of the four deaminated bases. Uridine cleavage may be vulnerable to amino acid substitutions because the enzyme primarily relies on two elements for its recognition. Any amino acid changes that exert an impact on element A or B, either directly or indirectly, may make it difficult to recognize the uridine and thus reduce its level of cleavage. Cleavage of oxanosine is incomplete with endonuclease V even when the enzyme is in excess, suggesting that the reactivity toward oxanosine is lower than toward the other deaminated bases (*9*). Tma endo V also fails to exhibit sufficiently strong binding affinity to be detected by gel mobility shift analysis (*9*). This may be explained by the interactions by recognition element B. For inosine, xanthosine, and uridine, element B may be accommodated by the bases without difficulty (Figure 8B). Furthermore, N^1 in inosine and xanthosine and N^3 in uridine are all hydrogen bond donors, which potentially may interact with element B by hydrogen bonding. On the other hand, interactions with oxanosine by element B are less ideal. The bulkier amino group at C^2 may present a steric hindrance that makes it less accommodating than other bases. The substitution of N^1 with O^1 converts it to a hydrogen bond acceptor, abolishing the complementarity in hydrogen bonding. Thus, an amino acid change in endonuclease V that affects DNA−protein interactions or active site organization in a subtle way may have a profound effect on oxanosine cleavage. According to these analyses, the deaminated bases can be recognized by three hydrogen bonding elements, two as donors in elements A and C and one as an acceptor in element B. Interestingly, the systematic site-directed mutagenesis analysis presented here implicates the hydrogen bonding capacity of the invariant Y80 and H116 residues in DNA−protein interactions. No obvious amino acid side chain emerged as a candidate for the hydrogen bond acceptor. However, one of the α-keto groups in the peptide backbone may offer such a functionality in the proposed base recognition scenario.

3′-Exonuclease Activity and Its Implication in Endonuclease V-Mediated Repair. One of the major findings from this work is the revelation of 3-exonuclease activity in endonuclease V (Figure 7). Although nonspecific cleavage was noticed in previous studies, it was thought that it may be caused by nonspecific endonuclease activity due to the observation that Tma endo V can cleave a circular plasmid (*2*). Triggered by our recent observation of Mn^{2+}-dependent nuclease activity (*9*), we set out to investigate whether the nonspecific cleavage bands are caused by exonuclease activity. Indeed, this work for the first time reveals that endonuclease V possesses 3′-exonuclease activity (Figure 7). Although the indication of 3′-exonuclease activity was not evident in the wt enzyme, it became definitively clear when the assays were performed using the mutants generated in this work. The binding effect may have caused the endo V mutants to pause and dissociate from the DNA more frequently, contributing to the formation of the ladder, typical of 3-exonuclease action (Figure 7).

Several hypothetical models have been put forward with regard to endonuclease V-mediated repair (*5*, *7*, *13*). Since endo V cleaves at the 3′ side one nucleotide downstream of the lesion, the DNA damage remains in the DNA after the endonuclease cleavage. It was proposed that a 3′-exonuclease (*5*, *7*, *13*) (Figure 8C) or an endonuclease (*13*) is needed to remove the lesion from the DNA. It has been suggested that APE1 or Mus81 may be involved in this process in mammalian systems (*5*). However, *E. coli* exonuclease III, which is a homologue of mammalian APE1, does not seem to be involved in the downstream process immediately after endo V cleavage (H. Gao and W. Cao, unpublished observation). *E. coli* DNA polymerase I, which contains 3′-exonuclease activity, and exo I 3′-exonuclease do not seem to be able to displace *E. coli* endo V from a nicked inosine substrate (H. Gao and W. Cao, unpublished observation).

Given the intrinsic 3′-exonuclease activity observed in endonuclease V, can endonuclease V in fact play a dual role in endonuclease V-initiated deamination repair? On the basis of the tight binding to the nicked inosine product, we have proposed that endonuclease V remains at the cleavage site to serve as a sensor to recruit other repairasome components for downstream processes (*2*, *10*). In light of the experimental evidence of 3′-exonuclease activity presented in this work, we infer that once the downstream protein(s) is recruited to the repair site by the endo V-nicked inosine DNA product complex, the protein−protein interactions between endo V and downstream protein(s) may induce a conformational change in endo V (Figure 8C). In this alternative model, endonuclease V switches from an endonuclease mode to a 3′-exonuclease mode, which progressively removes nucleotides from the 3′ side to the 5′ side and creates a gap for repair synthesis. This lesion removal process is similar to the function of MutS-MutL-MutH-ExoI in mismatch repair in *E. coli* (*22*). However, unlike the mismatch repair machinery which requires independent proteins and enzymes to recognize a mismatched base pair and fulfill distinct nucleolytic functions, a single enzyme, i.e., endonuclease V, is involved in deaminated lesion recognition, lesion specific endonucleolytic cleavage, and exonucleolytic lesion removal according to the model. As shown in Figure 8C, downstream proteins that interact with endo V may facilitate the mode switch that allows endo V to perform a dual enzymatic function in the repair pathway.

ACKNOWLEDGMENT

We thank Drs. Francis Barany and Jianmin Huang for providing R88E, R88Q, H116E, H116Q, H116T, and K139E overexpression clones. We also thank Thomas Hitchcock for helping with preparation of lesion-containing substrates and critically reading the manuscript.

REFERENCES

1. Yao, M., Hatahet, Z., Melamede, R. J., and Kow, Y. W. (1994) Purification and characterization of a novel deoxyinosine-specific enzyme, deoxyinosine 3′-endonuclease, from *Escherichia coli*, *J. Biol. Chem. 269*, 16260−8.
2. Huang, J., Lu, J., Barany, F., and Cao, W. (2001) Multiple Cleavage Activities of Endonuclease V from *Thermotoga maritima*: Recognition and Strand Nicking Mechanism, *Biochemistry 40*, 8738−48.
3. Yao, M., Hatahet, Z., Melamede, R. J., and Kow, Y. W. (1994) Deoxyinosine 3′-endonuclease, a novel deoxyinosine-specific endonuclease from *Escherichia coli*, *Ann. N.Y. Acad. Sci. 726*, 315−6.

4. Yao, M., and Kow, Y. W. (1997) Further characterization of *Escherichia coli* endonuclease V, *J. Biol. Chem. 272*, 30774−9.
5. Moe, A., Ringvoll, J., Nordstrand, L. M., Eide, L., Bjoras, M., Seeberg, E., Rognes, T., and Klungland, A. (2003) Incision at hypoxanthine residues in DNA by a mammalian homologue of the *Escherichia coli* antimutator enzyme endonuclease V, *Nucleic Acids Res. 31*, 3893−900.
6. Yao, M., and Kow, Y. W. (1995) Interaction of deoxyinosine 3′-endonuclease from *Escherichia coli* with DNA containing deoxyinosine, *J. Biol. Chem. 270*, 28609−16.
7. He, B., Qing, H., and Kow, Y. W. (2000) Deoxyxanthosine in DNA is repaired by *Escherichia coli* endonuclease V, *Mutat. Res. 459*, 109−14.
8. Kow, Y. W. (2002) Repair of deaminated bases in DNA, *Free Radical Biol. Med. 33*, 886−93.
9. Hitchcock, T. M., Gao, H., and Cao, W. (2004) Cleavage of deoxyoxanosine-containing oligodeoxyribonucleotides by bacterial endonuclease V, *Nucleic Acids Res. 32*, 4071−80.
10. Feng, H., Klutz, A. M., and Cao, W. (2005) Active Site Plasticity of Endonuclease V from *Salmonella typhimurium*, *Biochemistry 44*, 675−83.
11. Weiss, B. (2001) Endonuclease V of *Escherichia coli* prevents mutations from nitrosative deamination during nitrate/nitrite respiration, *Mutat. Res. 461*, 301−9.
12. Guo, G., and Weiss, B. (1998) Endonuclease V (nfi) mutant of *Escherichia coli* K-12, *J. Bacteriol. 180*, 46−51.
13. Burgis, N. E., Brucker, J. J., and Cunningham, R. P. (2003) Repair system for noncanonical purines in *Escherichia coli*, *J. Bacteriol. 185*, 3101−10.
14. Porello, S. L., Leyes, A. E., and David, S. S. (1998) Single-turnover and pre-steady-state kinetics of the reaction of the adenine glycosylase MutY with mismatch-containing DNA substrates, *Biochemistry 37*, 14756−64.
15. Waters, T. R., and Swann, P. F. (1998) Kinetics of the action of thymine DNA glycosylase, *J. Biol. Chem. 273*, 20007−14.
16. Huang, J., Lu, J., Barany, F., and Cao, W. (2002) Mutational analysis of endonuclease V from *Thermotoga maritima*, *Biochemistry 41*, 8342−50.
17. Ho, S. N., Hunt, H. D., Horton, R. M., Pullen, J. K., and Pease, L. R. (1989) Site-directed mutagenesis by overlap extension using the polymease chain reaction, *Gene 77*, 51−9.
18. Hitchcock, T. M., Dong, L., Connor, E. E., Meira, L. B., Samson, L. D., Wyatt, M. D., and Cao, W. (2004) Oxanine DNA glycosylase activity from mammalian alkyladenine glycosylase, *J. Biol. Chem. 279*, 38177−83.
19. Higgins, D. G., and Sharp, P. M. (1989) Fast and sensitive multiple sequence alignments on a microcomputer, *Comput. Appl. Biosci. 5*, 151−3.
20. Dalrymple, B. P., Kongsuwan, K., Wijffels, G., Dixon, N. E., and Jennings, P. A. (2001) A universal protein−protein interaction motif in the eubacterial DNA replication and repair systems, *Proc. Natl. Acad. Sci. U.S.A. 98*, 11627−32.
21. Lopez de Saro, F. J., and O'Donnell, M. (2001) Interaction of the β sliding clamp with MutS, ligase, and DNA polymerase I, *Proc. Natl. Acad. Sci. U.S.A. 98*, 8376−80.
22. Modrich, P., and Lahue, R. (1996) Mismatch repair in replication fidelity, genetic recombination, and cancer biology, *Annu. Rev. Biochem. 65*, 101−33.

BI050837C